Li, L., *et al.*: Numerical Simulation of Ultrasonic Heat Meter by Multiphysics ...
THERMAL SCIENCE: Year 2020, Vol. 24, No. 5B, pp. 3309-3317

3309

NUMERICAL SIMULATION OF ULTRASONIC HEAT METER BY MULTIPHYSICS COUPLING FINITE-ELEMENT SIMULATION SOFTWARE

by

Lin LI[a] and Hongliang ZHENG[b]*

[a] Department of Railway Signaling and Information Engineering,
Shandong Polytechnic, Jinan, Shandong, China
[b] School of Material Science and Engineering, Shandong University, Jinan, Shandong, China

Objective: To increase heat calculation accuracy, the numerical simulation of the ultrasonic heat meter is explored by multiphysics coupling. Methods: The COMSOL, a multiphysics coupling finite-element simulation software, is used to build the coupling model of the sound field, structure field, and electric field. The propagation of ultrasonic waves in heat meters is simulated, and its sound field distribution in pure water is analyzed. According to the operating conditions of ultrasonic heat meters, the influence of impurities with different concentrations on ultrasonic propagation is analyzed. The end-face sound pressure levels of the incident transducer and the receiving transducer are compared to obtain the attenuation laws of ultrasonic waves in the liquid-solid two-phase flow. Results: The main lobe and multiple side lobes exist during the propagation of ultrasonic waves. The energy of the main lobe is higher than that of the side lobes. Bubbles resonate under the action of the sound field. Also, bubbles of different diameters correspond to different resonance frequencies, which have larger sound pressure than that of the incident sound field. Most of the sound waves are reflected at the liquid-solid interface, while some of them continue to propagate through the media, affecting the sound pressure distribution on the end-face of the receiving transducer, thereby affecting the measurement accuracy of the ultrasonic heat meter. Conclusion: The reliability and detection efficiency of the heat meter is improved, which is significant and theoretically valuable.

Key words: *multiphysics coupling, finite element simulation software, ultrasonic heat meter, numerical simulation*

Introduction

With the rapid development of economy and technology, energy consumption in China continues to rise. Gradually, resources are in short supplies. Meanwhile, environmental problems are becoming increasingly severe. To solve the energy shortage and environmental pollution problems, in addition developing new energy, another powerful measure is energy saving and emission reducing [1]. For energy saving, developing energy-efficient buildings is one of the major tasks. Among the energies consumed by buildings, the heating system marks the majority. Especially, in Northern cities of China, with the popularity of heating systems, the proportion of heating consumption continues to rise [2].

---

* Corresponding author, e-mail: honglz@126.com

3310

Li, L., *et al.*: Numerical Simulation of Ultrasonic Heat Meter by Multiphysics ...
THERMAL SCIENCE: Year 2020, Vol. 24, No. 5B pp. 3309-3317

To ensure the smooth progress of the heating metering reform, developing a reliable and precise heat meter with low pressure loss and its corresponding detecting equipment has become the key [3]. At present, the research and development of the ultrasonic heat meter mainly focus on the circuit module of the totalizer that collects the ultrasonic signals. Scholars have investigated the circuit design of the ultrasonic heat meter that uses the time-difference measurement and temperature measurement. Also, scholars have proposed design solutions based on TDC-GP2 high-precision chips for flow measurement, temperature measurement, and low power consumption. Other scholars have applied CFD to explore the ultrasonic flowmeter with bends and obtained the velocity distribution in the pipes. Experiments have verified that numerical simulation calculation can analyze the design of ultrasonic flowmeter [4, 5]. The key to the transmission of ultrasonic measurement signals is the water flow characteristics in the base meter. Flow field analysis is the theoretical foundation of exploring the adaptability of the heat meter flow field. Understanding the flow field conditions in the base meter at different operating conditions is the core to solve the problems of heat meter flow measurement [6].

The accuracy of flow measurement in ultrasonic heat meters is the vital and difficult breakthrough in developing heat meters, which is affected by the following three aspects, *i. e.*, the way that heat meter circuit collects and processes the time difference signals, the influence of speed distribution in the base meter on correction coefficients, and the reliability of the detecting devices. Therefore, by referring to relevant technical data on ultrasonic heat meters worldwide, this study utilizes COMSOL, a multiphysics coupling finite-element simulation software, to build the coupling model of the sound field, structure field, and electric field. The propagation of ultrasonic waves in heat meters is simulated, and its sound field distribution in pure water is analyzed. According to the operating conditions of ultrasonic heat meters, the influence of impurities on ultrasonic propagation is analyzed. The end-face sound pressure levels of the incident transducer and the receiving transducer are compared to obtain the attenuation laws of ultrasonic waves in the liquid-solid two-phase flow. The influences of impurities on the measurement error of ultrasonic heat meters are explored from the acoustic aspect.

Methodology

Statistics show that in winter, heat-supply is mainly concentrated in Northern China, of which the centralized heat-supply of urban buildings reaches 2.52 billion m^2, accounting for 38% of the total building area in Northern cities and towns. The heating systems consume 130 millionns of standard coal annually, accounting for 20% of total energy consumption in Northern China. Compared with developed countries of the same climate, the heating energy consumption in China is tremendous. In addition the low-efficient heat-supply systems, the charging of heat-supply is another major cause of energy waste. Without household metering and charging, residents cannot regulate the heating and control the costs according to their needs, resulting in their weak energy-saving awareness. Moreover, once they leave the buildings, or they feel uncomfortable with the indoor temperature, residents cannot adjust the heating valves, thereby leading to severe energy waste [7, 8].

Measurement methods of ultrasonic heat meter

A heat meter, *i. e.*, thermal energy meter, is an instrument that measures heat [9]. It can measure both the heat supply and cold capacity. Generally, a heat meter consists of flow sensors, temperature sensors, and totalizers. Installing a heat meter includes installing a pair of temperature sensors on the inlet and outlet pipes and the flow sensors on the

Li, L., *et al.*: Numerical Simulation of Ultrasonic Heat Meter by Multiphysics ...
THERMAL SCIENCE: Year 2020, Vol. 24, No. 5B, pp. 3309-3317

3311

inlet or outlet pipes of the heat-supply system [10]. The temperature sensors measure the temperature of the inlet and outlet waters. The transducers in flow sensors send and receive ultrasonic waves. The totalizer calculates the temperature difference between the inlet and outlet waters, as well as the time difference between the propagation of ultrasonic waves in the forward and backward water flows. Therefore, the volume of flown fluid is obtained, and the heat is calculated:

$$Q = \int_0^T q_m \Delta h \mathrm{d}t \qquad (1)$$

where Q [kJ] is the released or absorbed heat, q_m [kgh^{-1}] – the fluid mass-flow, t [h] – the time, and Δh [kJkg^{-1}] – the specific enthalpy difference between the inlet and outlet of the heat cycling system.

In practical applications, the enthalpy difference cannot be directly measured by the device. Therefore, the K coefficient is often used in the measurement and calculation of heat meters. The K coefficient is a component function of hot water about the actual temperature. Through temperature compensation correction on the measurement results, it can improve the measurement accuracy of the heat meter significantly. Its measurement equation is shown:

$$Q = \int_{V_1}^{V_2} K \Delta \theta dq \qquad (2)$$

where Q [kJ] is the released heat, $\Delta \theta$ [°C] – the difference between the inlet and outlet of the heating supply, ΔV [m^3] – the volume of flown heating water, and K [kJm^{-3}°C^{-1}] – the heat coefficient, which is the function of heat-carrying fluid under corresponding temperature and pressure.

The framework of heat meter is shown in fig. 1.

An ultrasonic transducer is a sensor that converts electrical signals and ultrasonic signals mutually. This study uses a piezoelec-

Figure 1. Framework of heat meter

tric crystal ultrasonic transducer [11]. It converts energy according to the piezoelectric and inverse-piezoelectric effects between crystals. Piezoelectric effect refers to the polarization of a crystal once it receives an external force from a certain direction, at which both surfaces of the crystal, respectively, carry positive and negative charges [12]. Therefore, the ultrasonic transducer can convert ultrasonic signals into electrical signals. On the contrary, if the dielectric receives an electric field from a certain direction, it will undergo mechanical deformation, which is the inverse-piezoelectric effect. Mechanical vibration will drive the medium to radiate sound waves outward, thereby converting the electrical signals into ultrasonic signals [13]. The ultrasonic transducer is a device that converts electrical signals and ultrasonic signals mutually. Therefore, it has two operating states. When it is in the transmitting state, it converts electrical energy into sound energy for outward emission, which is the transmitting transducer. When it is in the receiving state, it converts the acoustic energy into electrical energy to receive ultrasonic signals, which is the receiving transducer [14].
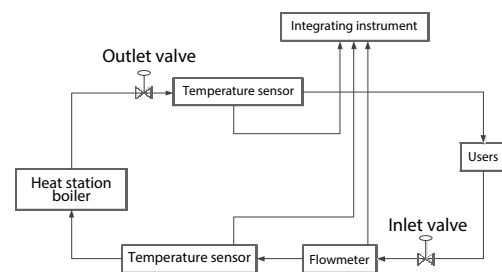
Finite-element simulation calculation
method based on Multiphysics coupling

In this study, the finite-element calculation involves the couplings among the physical fields of electricity, structure, and sound. The wave equation of the sound field:

$$\nabla\left(-\frac{1}{\rho_0}\nabla p\right)-\frac{\omega^2 p}{\rho_0 c^2}=0 \tag{3}$$

where p is the sound pressure, ρ_0 – the density of water (ρ_0 = 1000 kg/m^3), and c – the propagation velocity of sound waves in fluids (c = 1500 m/s). The equation of structural mechanics:

$$-\rho\omega^2 u-\nabla\sigma=F_V e^{i\phi} \tag{4}$$

where ρ is the density of piezoelectric material, u – the displacement of piezoelectric material, σ – the stress, F_V – the volume force, and $e^{i\phi}$ – the phase factor.
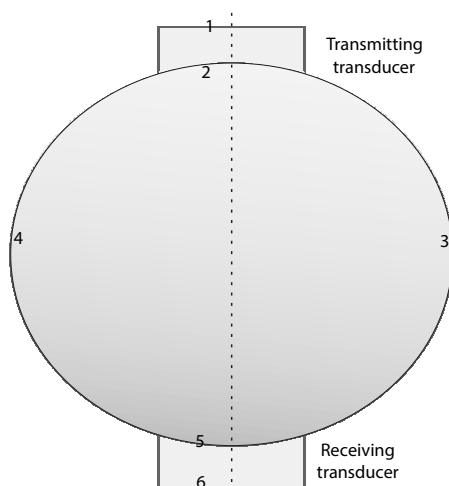

Figure 2. Calculation model

As shown in the calculation model of fig. 2, the calculation area is bilaterally symmetric. To reduce the calculation amount and accelerate the convergence rate, half of the calculation area is taken in the subsequent simulation process. The multiphysics coupling software COMSOL is used to build a 2-D symmetrical model. The pipe diameter is 20 mm.

The inner boundary – 2 of the transmitting transducer is set the voltage amplitude is 3.3 V, the frequency is 1 MHz, and the acoustic boundary condition is the structure-acoustic coupling. The outer boundary – 1 of the transmitting transducer is set the electrical boundary condition is structure-acoustic coupling, and the structural boundary condition is roller support. Other boundaries – 3-5 of the pipe walls are set the structural boundaries are free, and the acoustic boundary conditions of 3 and 4 are matching boundaries.

To ensure the accuracy of simulation calculations, the maximum grid size in the calculation domain is strictly controlled. For the calculation of acoustic waves, at least 6 grids are required in each wavelength range. Therefore, the maximum grid size is 1500 [ms^{-1}]/1000 [kHz]/6=0.25 mm, *i. e.*, the largest grid size is 0.2 mm.

Flow measurement is vital for the heat meter. The accuracy of the flow measurement directly determines the accuracy of the heat meter, as well as the success of the heat meter design [15]. Ultrasonic heat meter utilizes the principle of ultrasonic waves to measure flow. Specifically, the propagation velocity of the ultrasonic waves in the medium is affected by the flow velocity of the medium itself. Thus, the flow velocity of the medium is calculated by measuring the propagation velocity of the ultrasonic waves in the medium, thereby obtaining the volume flow rate. According to the different ultrasonic flow detection principles, the methods of ultrasonic flow detection include beam shift method, the Doppler method, correlation method, noise method, and time difference method.

Li, L., *et al.*: Numerical Simulation of Ultrasonic Heat Meter by Multiphysics ...
THERMAL SCIENCE: Year 2020, Vol. 24, No. 5B, pp. 3309-3317

3313

This study uses the time difference method. In a flowing medium, the propagation velocity of the ultrasonic waves will change due to the flowing direction of the medium, which will increase in the forward direction and decrease in the backward direction. Therefore, the medium velocity is calculated by measuring the difference between the propagation time of the ultrasonic waves in the forward and backward flows of the medium.

Results

Numerical simulation results of ultrasonic heat meter

Given the stable flow rate, at a small flow $Q = 0.07$ m^3/h, the k coefficient is small. With the increase in flow rate, the k coefficient increases. After $Q = 0.35$ m^3/h, the changes in the k coefficient become slight and tend to a horizontal line.

The flow rate reaches a steady-state after the valve is opened. During the period, the linear average speed measured by the flow sensors is constant. However, in previous designs of heat meters, the coefficient used in this period is the same as that in the steady-state. Since the coefficient is different from that in the flow changing process, flow measurement errors occur. To compare the influence of flow correction coefficient on flow measurement during steady-state and the open valve, the flow rates corrected by unsteady simulation coefficients and steady-state coefficients are calculated, respectively.

Once the valve is opened, due to the continuous increase in flow rate, at the small flow rate points, the flowing state in the base meter of the heat meter is not a typical laminar flow. Also, the current k coefficient is larger than that at a steady flow state. As the flow rate increases, the k coefficient becomes larger. Meanwhile, compared with that at steady-state, the k coefficient is no longer a horizontal line. Instead, it increases as the flow points increase. As the flow rate gradually stabilizes, the k coefficient tends to stable, and its value is consistent with the steady flow state. The coefficient changes of the ultrasonic heat meter in the unsteady-state can provide theoretical guidance for the flow correction during the valve opening or closing process. It is significant for improving the measurement accuracy of the heat meter under various operating conditions. Figure 3 shows the comparison of k coefficient changes between steady-state and open-valve. Figure 4 shows the comparison of changes in average speed after opening the valve.
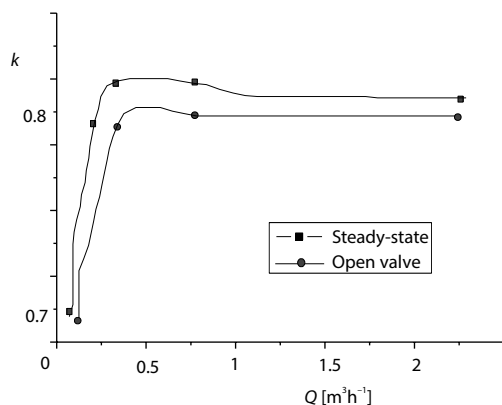
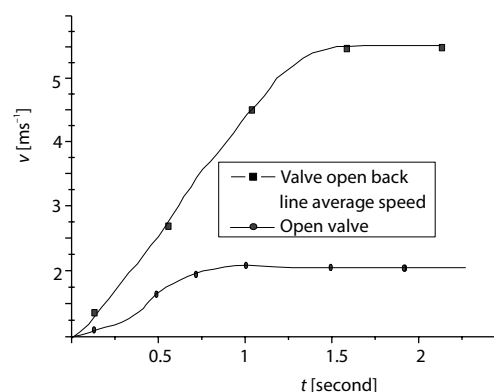**Figure 3. Comparison of k coefficient changes between steady-state and open-valve**

Figure 4. Comparison of changes in average speed after opening the valve

3314

Li, L., *et al.*: Numerical Simulation of Ultrasonic Heat Meter by Multiphysics ...
THERMAL SCIENCE: Year 2020, Vol. 24, No. 5B pp. 3309-3317

Influences of impurities on measurement
errors of ultrasonic heat meters

Under the actions of the voltage across the ultrasonic transducer, the ultrasonic transducer generates mechanical vibration convert electrical energy into mechanical energy, thereby emits ultrasonic waves. The energy of ultrasound is concentrated on the central axis, *i. e.*, the main lobe area. For an ultrasonic transducer in which the piezoelectric wafer is a cylinder, multiple side lobes exist in addition the main lobe area. Compared with the main lobe, and the energy of the side lobes is smaller.

When sound waves propagate in pure water, due to the equal acoustic impedance everywhere, sound scattering will not occur. However, when sound waves propagate in water containing impurities, due to the different acoustic characteristics of the fluid medium and the particles, acoustic scattering occurs during the propagation of the sound waves, which makes the sound propagation problem complicated. This study chooses bubbles with four diameters of 0.1 mm, 0.2 mm, 0.3 mm, and 0.4 mm. The scattering field of a single bubble is calculated to verify the accuracy of the simulation.

Figure 5 shows the correlation between the sound pressure and frequency at for a single bubble with four different diameters (0.4 mm, 0.3 mm, 0.2 mm, 0.1 mm). As shown in fig. 5, spherical bubbles with four different diameters all resonate, among which the resonance frequency of $D = 0.1$ mm bubble is 65.632 kHz, the resonance frequency of $D = 0.2$ mm bubble is 32.836 kHz, the resonance frequency of $D = 0.3$ mm bubble is 21.853 kHz, and the resonance frequency of $D = 0.4$ mm bubble is 16.411 kHz. The sound pressure value when the bubble resonates is much larger than that when no resonance occurs. Bubbles with different diameters correspond to different resonance frequencies, and the resonance frequency decreases as the bubble diameter increases.
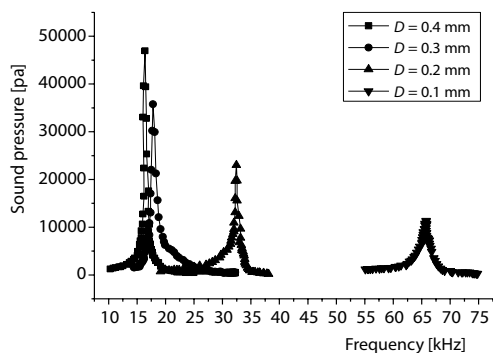

Figure 5. The correlation of sound pressure with frequency

Under the actions of sound waves, accompanied by volume vibrations, bubbles in fluid media generate periodic expansion and compression. These bubbles are equivalent to simple harmonic oscillators. If the frequency of the incident sound wave is the same as the natural oscillation frequency of the bubbles, the bubble resonance will be the most apparent, and the resonance frequency is calculated:

$$f_{\text{minnaert}} = \frac{1}{\pi D} \sqrt{\frac{3\gamma p_0}{\rho_L}} \tag{5}$$

where D is the diameter of the bubble, p_0 – the static pressure (p_0=101325 Pa), γ – the specific heat capacity of the gas, in the adiabatic state ($\gamma = 1.4$), and ρ_L – the fluid medium density around the bubble, which takes the density of water as ρ_L =1000 kg/m³. Taking the bubble of $D = 0.1$ mm as an example, the resonance frequency obtained by simulation is 65.632 kHz, and the analytical solution obtained by eq. (5) is 65.698 kHz.

When a bubble resonates, its resonant sound pressure is greater than that of the incident sound wave. During resonance, the maximum sound pressure can reach 19 kPa, while the incident sound pressure used in the calculation process is only 1 kPa, *i. e.*, the incident sound

Li, L., *et al.*: Numerical Simulation of Ultrasonic Heat Meter by Multiphysics ...
THERMAL SCIENCE: Year 2020, Vol. 24, No. 5B, pp. 3309-3317

3315

field slightly affects the total sound field. Currently, the resonating bubbles continuously emit energy outward, affecting the sound field distribution around the bubbles.

In the practical applications of ultrasonic heat meters, water often contains various impurities. Besides, the filters installed in the major pipe network cannot remove the impurities whose particle sizes are close to ultrasonic wavelength. Therefore, this study builds a liquid-solid two-phase flow model in the ultrasonic heat meter by placing circular iron particles with a radius of 0.1 mm evenly on the lower side of the pipe. Another spatial medium is water. The influences of impurities on the propagation of ultrasonic waves at different concentrations are analyzed.

As shown in fig. 6, when the particle concentration changes between 0% and 3.5%, in the liquid-solid two-phase flow, the attenuation rate of sound pressure level changes between 0% and 7%. Given 1 MHz transmitting frequency of the ultrasonic transducer, the attenuation rate of the sound pressure level at the receiving end fluctuates around 4%. Such changes are disordered without apparent laws. According to the definition of acoustic impedance $Z = \rho c$ (where ρ is the medium density and c is the sound velocity in the medium), the acoustic impedance of water and iron at 20 °C is $1.5 \cdot 10^6$ Pa·s/m and $4.466 \cdot 10^7$ Pa·s/m, respectively. Therefore, the acoustic reflectivity $R = 0.8742$ at the interface between both media is obtained, *i. e.*, most of the sound waves are reflected at the interface, while some waves continue to propagate through the iron. Consequently, the sound pressure at the end-face of the receiving transducer changes, which affects the measurement accuracy of the heat meter.
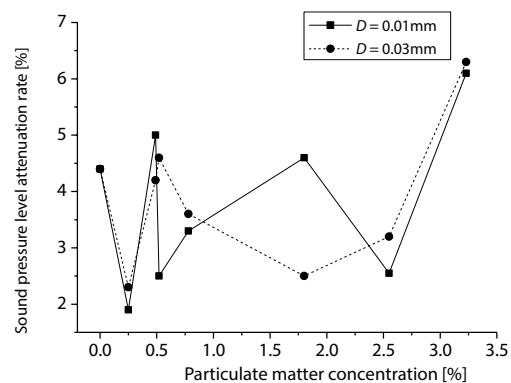

Figure 6. Attenuation rates of sound pressure level at different impurity concentrations

Discussion

To solve the energy shortage and environmental pollution problems, in addition developing new energy, another powerful measure is energy saving and emission reducing. Heat-supply is the major cause of energy waste and environmental pollution. The traditional area-based charging of heat-supply is the main reason for heat waste. The only solution the resource-wasting problem is household metering and charging of heat-supply, which charges the fee according to the heat consumption. Such a solution not only prevents resource-wasting but also makes residents understand their energy consumption clearer. To implement this solution, heat meters with excellent performance are necessary. This study explores several issues affecting the measurement accuracy of ultrasonic heat meters.

This study combines theoretical analysis and numerical simulation. By utilizing COMSOL, a multiphysics coupling finite-element simulation software, this study builds a coupling model of the sound field, structure field, and electric field. The propagation of ultrasonic waves in heat meters is simulated, and its sound field distribution in pure water is analyzed. According to the operating conditions of ultrasonic heat meters, the influence of impurities with different concentrations on ultrasonic propagation is analyzed. The end-face sound pressure levels of the incident transducer and the receiving transducer are compared to obtain the attenuation laws of ultrasonic waves in the liquid-solid two-phase flow. The influences of impurities on the

3316

Li, L., *et al.*: Numerical Simulation of Ultrasonic Heat Meter by Multiphysics ...
THERMAL SCIENCE: Year 2020, Vol. 24, No. 5B pp. 3309-3317

measurement error of ultrasonic heat meters are explored from the acoustic aspect. This study analyzes factors affecting the accuracy and performance of flow measurement by ultrasonic heat meters. Starting from the processing of the collected time difference signals, the water flow characteristics in the base meter, the reliability of the detecting device, and the valve opening process, this study investigates the impacts of these factors on the performance of the base meter of the ultrasonic heat meter. Consequently, this study proposes corresponding solutions.

Conclusion

By coupling the physical fields of electricity, structure, and sound, the propagation of ultrasonic waves in pipes is simulated, and the distribution of ultrasonic waves in pure water is obtained. The main lobe and multiple side lobes exist during the propagation of ultrasonic waves. The energy of the main lobe is higher than that of the side lobes. The sound scattering field of a single bubble is explored. Bubbles resonate under the action of the sound field. Also, bubbles of different diameters correspond to different resonance frequencies, which have larger sound pressure than that of the incident sound field. Changes in the sound pressure level attenuation rate of ultrasonic waves are disordered in the liquid-solid two-phase flow. Most of the sound waves are reflected at the liquid-solid interface, while some of them continue to propagate through the media, affecting the sound pressure distribution on the end-face of the receiving transducer, thereby affecting the measurement accuracy of the ultrasonic heat meter. Meanwhile, there are also improvements to be made on the research contents of this study. For example, the water flow velocity can be controlled and kept within a stable range to facilitate calculations. Also, practical situations should be investigated. Most of the analyses in this study are simulation results in the theoretical stage. Corresponding explorations in practical applications can guarantee the requirements.

References

[1] Bungartz, H. J., *et al.*, preCICE – A fully Parallel Library for Multi-Physics Surface Coupling, *Computers and Fluids*, *141* (2016), Dec., pp. 250-258
[2] Zhou, Y. P., *et al.*, The Effect of the Full-Spectrum Characteristics of Nanostructure on the PV-TE Hybrid System Performances within Multi-Physics Coupling Process, *Applied Energy*, *213* (2018), Mar., pp. 169-178
[3] Pan, Z., *et al.*, Aircraft Pulsating Assembly Line Balancing Problem Based on Hybrid Algorithm, *Computer Integrated Manufacturing Systems*, *24* (2018), 10, pp. 2436-2447
[4] Shaofei, W., Study and Evaluation of Clustering Algorithm for Solubility and Thermodynamic Data of Glycerol Derivatives, *Thermal Science*, 23 (2019), 5, pp. 2867-2875
[5] Miehe, C., *et al.*, Phase Field Modelling of Fracture in Multi-Physics Problems – Part II: Coupled Brittle-to-Ductile Failure Criteria and Crack Propagation in Thermo-Elastic-Plastic Solids, *Computer Methods in Applied Mechanics and Engineering*, *294* (2015), Sept., pp. 486-522
[6] Poulet, T., *et al.*, Multi-Physics Modelling of Fault Mechanics Using Redback: A Parallel Open-Source Simulator for Tightly Coupled Problems, *Rock Mechanics and Rock Engineering*, *50* (2017), Mar., pp. 733-749
[7] Zhou, Y. P., *et al.*, Multi-Physics Analysis: The Coupling Effects of Nanostructures on the Low Concentrated Black Silicon Photovoltaic System Performances, *Energy Conversion and Management*, *159* (2018), Mar., pp. 129-139
[8] Davis, I., *et al.*, High-Fidelity Multi-Physics Coupling for Determination of Hydride Distribution in Zr-4 cladding, *Annals of Nuclear Energy, 110* (2017), Dec., pp. 475-485
[9] Shaofei, W., *et al.*, Bidirectional Cognitive Computing Method Supported by Cloud Technology, *Cognitive Systems Research*, *52* (2018), Dec., pp. 615-621
[10] Zheng, M., *et al.*, Ultrasonic Heat Transfer Enhancement on Different Structural Tubes in LiBr Solution, *Applied Thermal Engineering*, *106* (2016), Aug., pp. 625-633

[11] Cordova, L., *et al.*, Qualification of an Ultrasonic Flow Meter as a Transfer Standard for Measurements at Reynolds Numbers up to 4×106 between NMIJ and PTB, *Flow Measurement and Instrumentation*, *45* (2015), Oct., pp. 28-42

[12] Liu, E., *et al.*, A CFD Simulation for the Ultrasonic Flow Meter with a Header, *Tehnicki Vjesnik-Technical Gazette*, *24* (2017), 6, pp. 1797-1802

[13] Tam, H. K., *et al.*, Experimental Study of the Ultrasonic Effect on Heat Transfer Inside a Horizontal Mini-tube in the Laminar Region, *Applied Thermal Engineering*, *114* (2017), Mar., pp. 1300-1308

[14] Zhang, L., Chen, Z. J., Design and Research of the Movable Hybrid Photo-voltaic-Thermal (PVT) System, *Energies*, *10* (2017), 4, 507

[15] Nagaso, M., *et al.*, Ultrasonic Thermometry Simulation in a Random Fluctuating Medium: Evidence of the Acoustic Signature of a One-Percent Temperature Difference, *Ultrasonics*, *68* (2016), May, pp. 61-70